Nonlinear Multidimensional Spectroscopy

Blaise Thompson

University of Wisconsin–Madison

2017-11-07

Chemical systems

chemical systems are complex!

- many molecules
  - 10^{25} in a cup of coffee
  - 1 trillion in each human cell
- multiple interaction modes
- potential for very rare but important species (*e.g.* catalysts)
- dynamics and equilibrium

Dynamics

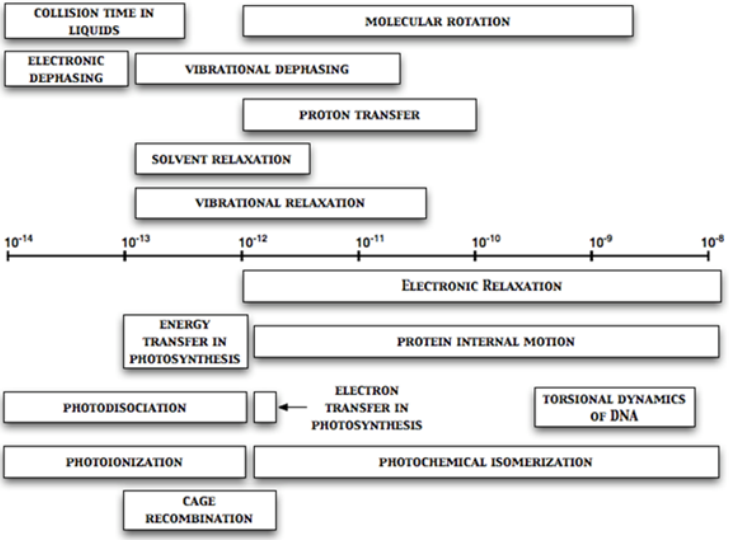
COLLISION TIME IN LIQUIDS
MOLECULAR ROTATION
ELECTRONIC DEPHASING
VIBRATIONAL DEPHASING
PROTON TRANSFER
SOLVENT RELAXATION
VIBRATIONAL RELAXATION
10^{-14}
10^{-13}
10^{-12}
10^{-11}
10^{-10}
10^{-9}
10^{-8}
ELECTRONIC RELAXATION
ENERGY TRANSFER IN PHOTOSYNTHESIS
PROTEIN INTERNAL MOTION
PHOTODISOCIATION
ELECTRON TRANSFER IN PHOTOSYNTHESIS
TORSIONAL DYNAMICS OF DNA
PHOTOIONIZATION
PHOTOCHEMICAL ISOMERIZATION
CAGE RECOMBINATION

Analytical chemistry

analytical chemists separate, identify, and quantify chemical systems

to do this, we build instruments that exploit physical properties of the component molecules

- separation (chromatography, electrophoresis)
- mass spectrometry
- electrochemistry
- microscopy
- spectroscopy

as a spectroscopist, I focus on ways to exploit **light matter interaction**

Spectroscopy

molecules respond to electric fields

static electric fields cause charged molecules (ions) to move, as in electrophoresis and mass spectrometry

oscillating electric fields (light) can interact directly with the molecules themselves, driving **transitions** within the molecule

however, these transitions can only be driven with the appropriate frequency of light (resonance)

different frequencies (colors) of light interact with different kinds of transitions, revealing different features of the molecule of interest

Spectroscopy

energy range	transition
radio	nuclear
microwave	rotational
IR	vibrational
visible	electronic
UV	electronic
X-rays	buried electronic (elemental)

Spectroscopy

video: how is a photon created or absorbed?

Nonlinear Spectroscopy

spectroscopy is fantastic, but sometimes simple experiments don't reveal everything

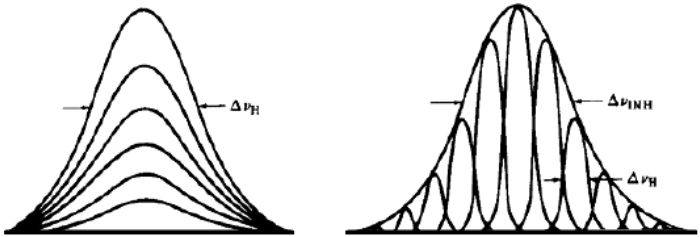

Homogeneous (a) and inhomogeneous (b) band shapes having inhomogeneous width $\Delta\nu_{INH}$ and homogeneous width $\Delta\nu_H$

nonlinear spectroscopy exploits nonlinearity (multi-photon) interactions to further decongest the spectrum

Nonlinear Spectroscopy

in a simple case like resolving inhomogeneous broadening, multidmensional spectroscopy can be thought of as a measurement of the correlation function

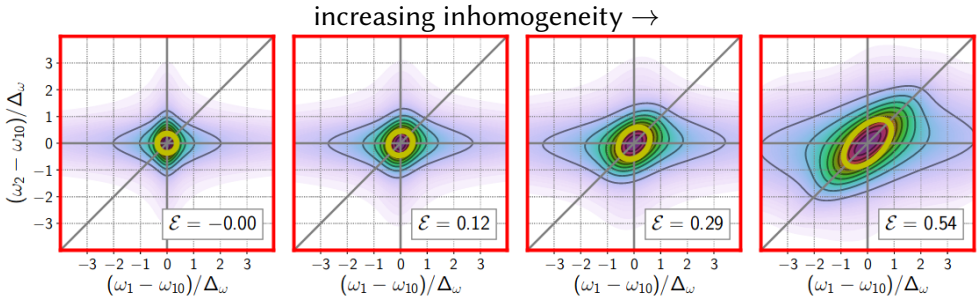

Instrumentation

to accomplish nonlinear spectroscopy, specialized light sources are needed

- gigantic electric fields
- ultrafast time resolution
- tunable frequencies

Nonlinear Multidimensional Spectroscopy

Blaise Thompson

Chemical systems

Analytical chemistry

Spectroscopy

Instrumentation

LASER

OPA

Experiment

Gasses

Drug complexing

Quantum dots

Conductive polymers

Original LASER

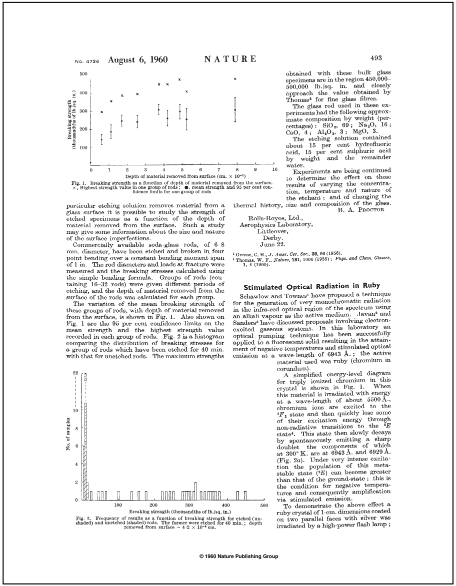

obtained with these bulk glass specimens are in the region 450,000–500,000 lb./sq. in. and closely approach the value obtained by Thomas[2] for fine glass fibres.

The glass rod used in these experiments had the following approximate composition by weight (percentages): SiO_2, 69; Na_2O, 16; CaO, 4; Al_2O_3, 3; MgO, 3.

The etching solution contained about 15 per cent hydrofluoric acid, 15 per cent sulphuric acid by weight and the remainder water.

Experiments are being continued to determine the effect on these results of varying the concentration, temperature and nature of the etchant; and of changing the thermal history, size and composition of the glass.

Fig. 1. Breaking strength as a function of depth of material removed from the surface. ×, Highest strength value in one group of rods; ●, mean strength and 95 per cent confidence limits for one group of rods

particular etching solution removes material from a glass surface it is possible to study the strength of etched specimens as a function of the depth of material removed from the surface. Such a study may give some information about the size and nature of the surface imperfections.

Commercially available soda-glass rods, of 6–8 mm. diameter, have been etched and broken in four point bending over a constant bending moment span of 1 in. The rod diameters and loads at fracture were measured and the breaking stresses calculated using the simple bending formula. Groups of rods (containing 16–32 rods) were given different periods of etching, and the depth of material removed from the surface of the rods was calculated for each group.

The variation of the mean breaking strength of these groups of rods, with depth of material removed from the surface, is shown in Fig. 1. Also shown on Fig. 1 are the 95 per cent confidence limits on the mean strength and the highest strength value recorded in each group of rods. Fig. 2 is a histogram comparing the distribution of breaking stresses for a group of rods which have been etched for 40 min. with that for unetched rods. The maximum strengths

Fig. 2. Frequency of results as a function of breaking strength for etched (unshaded) and unetched (shaded) rods. The former were etched for 40 min.; depth removed from surface = $4 \cdot 2 \times 10^{-2}$ cm.

B. A. PROCTOR

Rolls-Royce, Ltd.,
Aerophysics Laboratory,
Littleover,
Derby.
June 22.

[1] Greene, C. H., *J. Amer. Cer. Soc.*, **39**, 66 (1956).
[2] Thomas, W. F., *Nature*, **181**, 1006 (1958); *Phys. and Chem. Glasses*, **1**, 4 (1960).

Stimulated Optical Radiation in Ruby

Schawlow and Townes[1] have proposed a technique for the generation of very monochromatic radiation in the infra-red optical region of the spectrum using an alkali vapour as the active medium. Javan[2] and Sanders[3] have discussed proposals involving electron-excited gaseous systems. In this laboratory an optical pumping technique has been successfully applied to a fluorescent solid resulting in the attainment of negative temperatures and stimulated optical emission at a wave-length of 6943 Å.; the active material used was ruby (chromium in corundum).

A simplified energy-level diagram for triply ionized chromium in this crystal is shown in Fig. 1. When this material is irradiated with energy at a wave-length of about 5500 Å., chromium ions are excited to the $^4F_2$ state and then quickly lose some of their excitation energy through non-radiative transitions to the ^2E state[4]. This state then slowly decays by spontaneously emitting a sharp doublet the components of which at 300° K. are at 6943 Å. and 6929 Å. (Fig. 2*a*). Under very intense excitation the population of this metastable state (^2E) can become greater than that of the ground-state; this is the condition for negative temperatures and consequently amplification via stimulated emission.

To demonstrate the above effect a ruby crystal of 1-cm. dimensions coated on two parallel faces with silver was irradiated by a high-power flash lamp;

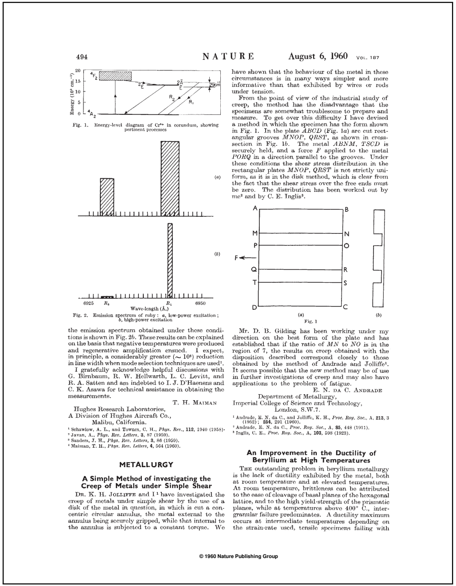

Fig. 1. Energy-level diagram of Cr^{3+} in corundum, showing pertinent processes

Fig. 2. Emission spectrum of ruby: *a*, low-power excitation; *b*, high-power excitation

the emission spectrum obtained under these conditions is shown in Fig. 2*b*. These results can be explained on the basis that negative temperatures were produced and regenerative amplification ensued. I expect, in principle, a considerably greater ($\sim 10^8$) reduction in line width when mode selection techniques are used[1].

I gratefully acknowledge helpful discussions with G. Birnbaum, R. W. Hellwarth, L. C. Levitt, and R. A. Satten and am indebted to I. J. D'Haenens and C. K. Asawa for technical assistance in obtaining the measurements.

T. H. MAIMAN

Hughes Research Laboratories,
A Division of Hughes Aircraft Co.,
Malibu, California.

[1] Schawlow, A. L., and Townes, C. H., *Phys. Rev.*, **112**, 1940 (1958).
[2] Javan, A., *Phys. Rev. Letters*, **3**, 87 (1959).
[3] Sanders, J. H., *Phys. Rev. Letters*, **3**, 86 (1959).
[4] Maiman, T. H., *Phys. Rev. Letters*, **4**, 564 (1960).

METALLURGY

A Simple Method of investigating the Creep of Metals under Simple Shear

DR. K. H. JOLLIFFE and I[1] have investigated the creep of metals under simple shear by the use of a disk of the metal in question, in which is cut a concentric circular annulus, the metal external to the annulus being securely gripped, while that internal to the annulus is subjected to a constant torque. We have shown that the behaviour of the metal in these circumstances is in many ways simpler and more informative than that exhibited by wires or rods under tension.

From the point of view of the industrial study of creep, the method has the disadvantage that the specimens are somewhat troublesome to prepare and measure. To get over this difficulty I have devised a method in which the specimen has the form shown in Fig. 1. In the plate *ABCD* (Fig. 1*a*) are cut rectangular grooves *MNOP*, *QRST*, as shown in cross-section in Fig. 1*b*. The metal *ABNM*, *TSCD* is securely held, and a force *F* applied to the metal *PORQ* in a direction parallel to the grooves. Under these conditions the shear stress distribution in the rectangular plates *MNOP*, *QRST* is not strictly uniform, as it is in the disk method, which is clear from the fact that the shear stress over the free ends must be zero. The distribution has been worked out by me[2] and by C. E. Inglis[3].

Fig. 1

Mr. D. B. Gilding has been working under my direction on the best form of the plate and has established that if the ratio of *MN* to *NO* is in the region of 7, the results on creep obtained with the disposition described correspond closely to those obtained by the method of Andrade and Jolliffe[1]. It seems possible that the new method may be of use in further investigations of creep and may also have applications to the problem of fatigue.

E. N. DA C. ANDRADE

Department of Metallurgy,
Imperial College of Science and Technology,
London, S.W.7.

[1] Andrade, E. N. da C., and Jolliffe, K. H., *Proc. Roy. Soc.*, A, **213**, 3 (1952); **254**, 291 (1960).
[2] Andrade, E. N. da C., *Proc. Roy. Soc.*, A, **85**, 448 (1911).
[3] Inglis, C. E., *Proc. Roy. Soc.*, A, **103**, 598 (1923).

An Improvement in the Ductility of Beryllium at High Temperatures

THE outstanding problem in beryllium metallurgy is the lack of ductility exhibited by the metal, both at room temperature and at elevated temperatures. At room temperature, brittleness can be attributed to the ease of cleavage of basal planes of the hexagonal lattice, and to the high yield-strength of the prismatic planes, while at temperatures above 400° C., intergranular failure predominates. A ductility maximum occurs at intermediate temperatures depending on the strain-rate used, tensile specimens failing with

Original LASER

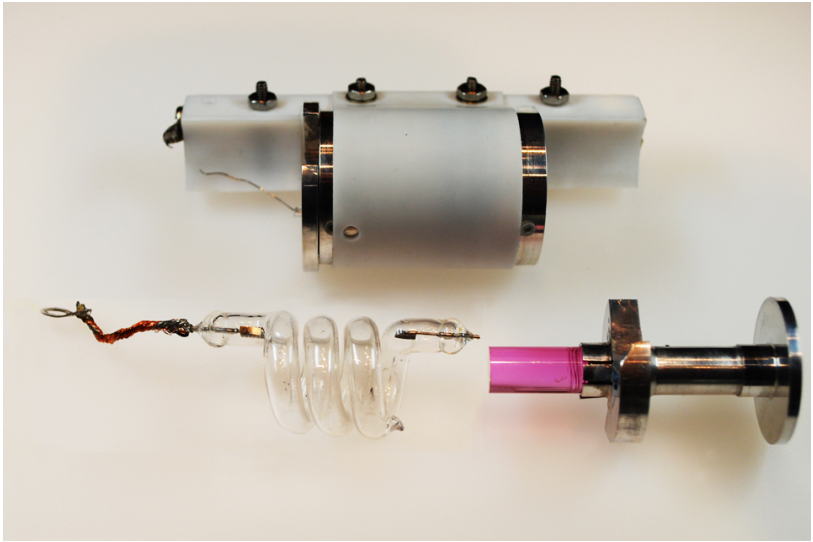

Original LASER

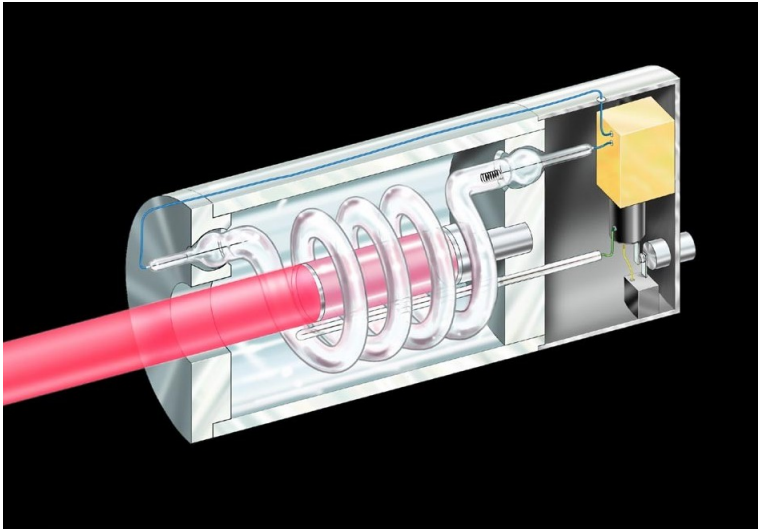

LASER

LASERs are **coherent**

- spatially
- temporally

Temporal coherence

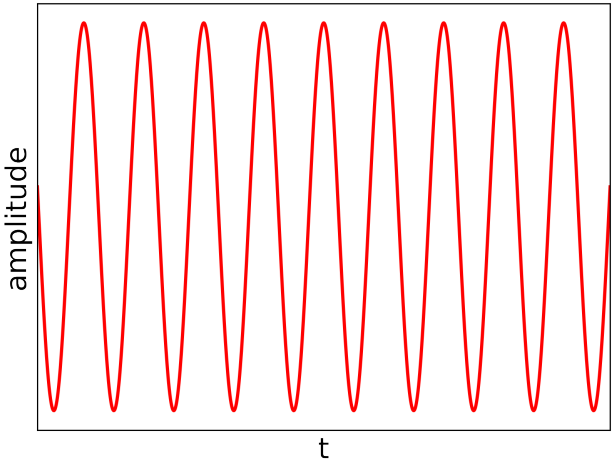

Pulse

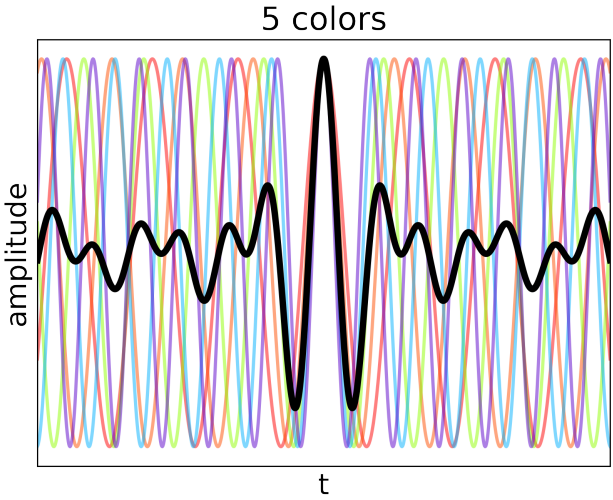

Pulse

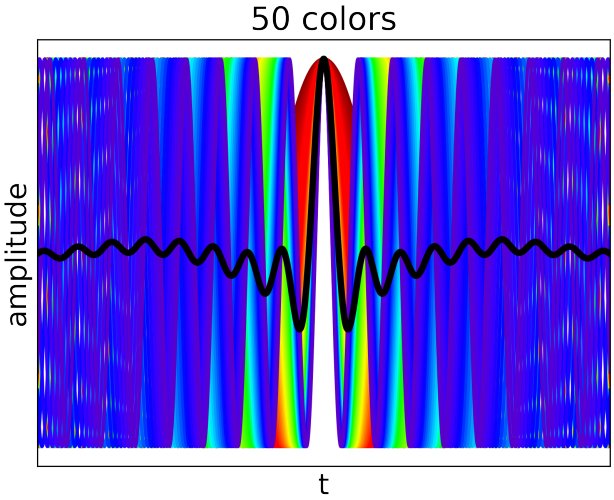

LASER

by keeping a wide range of colors in phase simultaniously, we are able to create **ultrafast** pulses of light

in my case

- 35×10^{-15} full width half maximum
- 1 KHz rep rate

very short

fun fact:

$$\frac{\text{pulse duration (35 fs)}}{\text{time between pulses (1 ms)}} \approx \frac{\text{5.75 months}}{\text{age of universe (13.7 billion years)}}$$

proportionally, our sample spends 6 months in the “sun” for every age of the universe in the dark

very intense

fun fact:

$$\frac{\text{energy per pulse (4 mJ)}}{\text{pulse duration (35 fs)}} \approx \frac{\text{US electricity generation } (5.43 \times 10^{11}\ \text{W})}{5}$$

our laser outputs electric fields one fifth as powerful as total US electricity generation (2016)

LASER

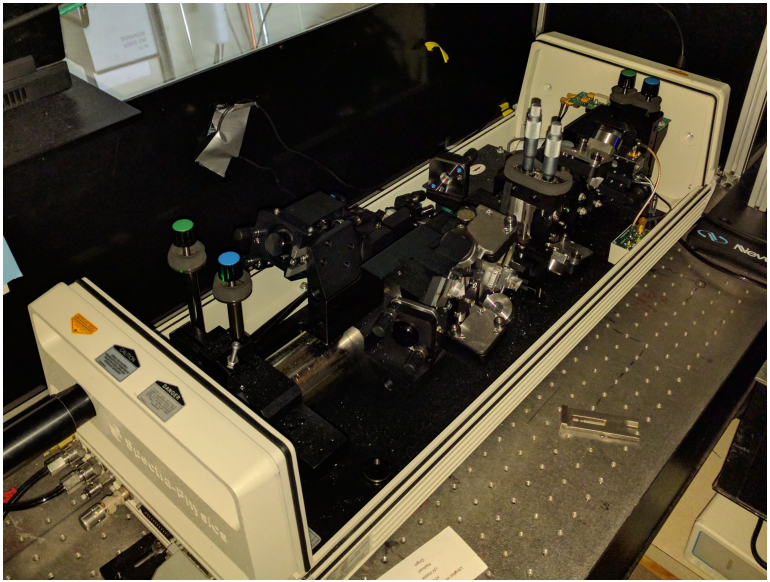

LASER

ultrafast lasers are used for more than just spectroscopy

- fs lasers are used for bladeless surgery, such as LASIK eye surgery
- ultrafast lasers are key to inertial confinement fusion devices, such as the National Ignition Facility
- precision machining (ablation without heating)
- microscopy

REVIEW OF SCIENTIFIC INSTRUMENTS VOLUME 74, NUMBER 1 JANUARY 2003

REVIEW ARTICLE

Ultrafast optical parametric amplifiers

Giulio Cerullo and Sandro De Silvestri[a)]
Istituto Nazionale per la Fisica della Materia, IFN-CNR, Dipartimento di Fisica, Politecnico, I-20133 Milano, Italy

(Received 26 October 2001; accepted 27 July 2002)

Over the last decade there have been spectacular developments in ultrafast laser technology, due to the introduction of solid state active materials and of new mode-locking and amplification techniques. These advances, together with the discovery of new nonlinear optical crystals, have fostered the introduction of ultrafast optical parametric amplifiers as a practical source of femtosecond pulses tunable across the visible and infrared spectral ranges. This article summarizes the recent progress in the development of ultrafast optical parametric amplifiers, giving the basic design principles for different frequency ranges and in addition presenting some advanced designs for the generation of ultrabroadband, few-optical-cycle pulses. Finally, we also briefly discuss the possibility of applying parametric amplification schemes to large-scale, petawatt-level systems. [DOI: 10.1063/1.1523642]

I. INTRODUCTION

Ultrafast optical science is a rapidly evolving multidisciplinary field: the ability to excite matter with femtosecond magnitude, from the millijoule to the multijoule level. This increase in peak power makes it possible to access a whole new class of nonlinear optical phenomena, triggering a renaissance in the field of nonlinear optics. Parallel to these

OPA

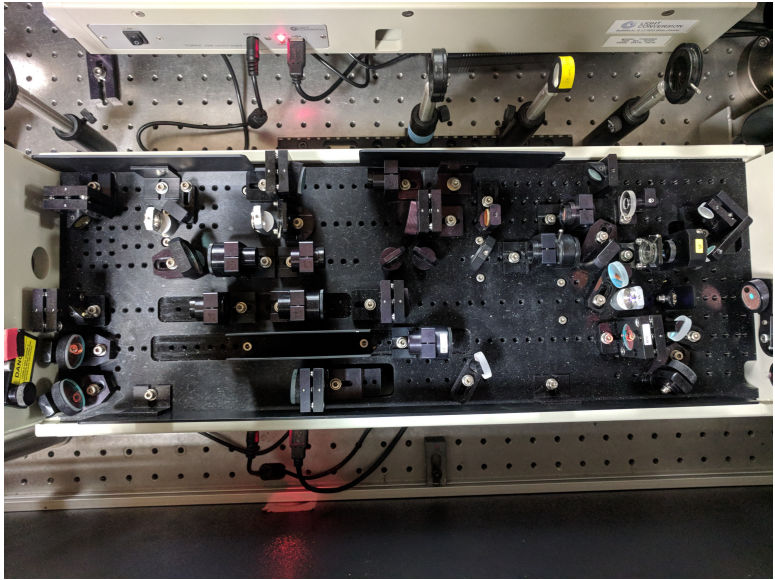

OPA

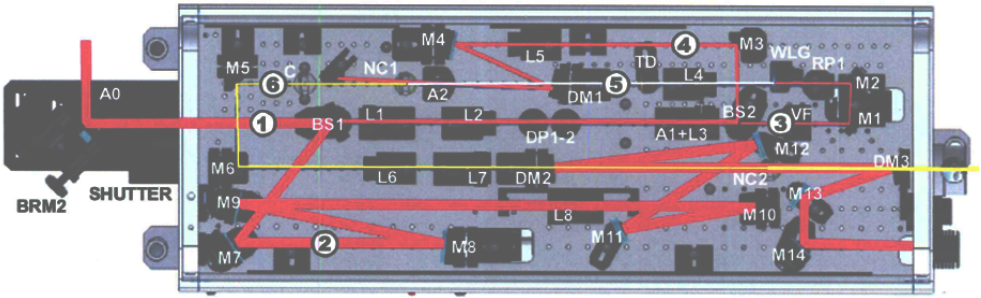
A0
BRM2
SHUTTER
M4
L5
M3
WLG
RP1
M5
C
NC1
TD
L4
M2
A2
DM1
BS2
VF
M1
BS1
L1
L2
DP1-2
A1+L3
M12
DM3
M6
L6
L7
DM2
NC2
M13
M9
L8
M10
M11
M7
M8
M14
1
2
3
4
5
6

OPA

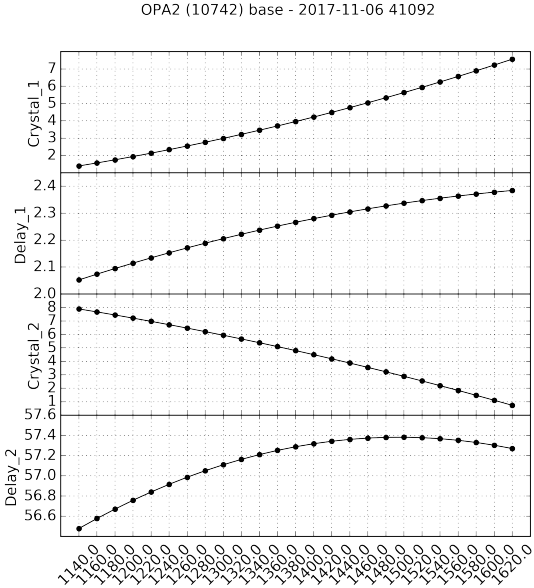
OPA2 (10742) base - 2017-11-06 41092
Crystal_1
Delay_1
Crystal_2
Delay_2
1140.0
1160.0
1180.0
1200.0
1220.0
1240.0
1260.0
1280.0
1300.0
1320.0
1340.0
1360.0
1380.0
1400.0
1420.0
1440.0
1460.0
1480.0
1500.0
1520.0
1540.0
1560.0
1580.0
1600.0
1620.0

OPA

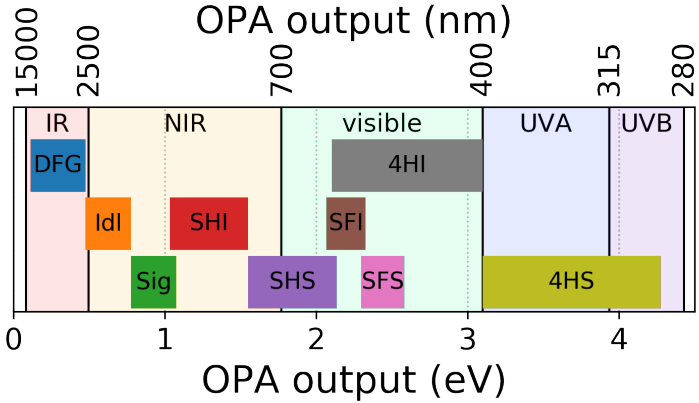
OPA output (nm)
15000
2500
700
400
315
280
IR
NIR
visible
UVA
UVB
DFG
4HI
IdI
SHI
SFI
Sig
SHS
SFS
4HS
0
1
2
3
4
OPA output (eV)

JOURNAL OF CHEMICAL PHYSICS VOLUME 110, NUMBER 12 22 MARCH 1999

Femtosecond transient-grating techniques: Population and coherence dynamics involving ground and excited states

Emily J. Brown, Qingguo Zhang,[a] and Marcos Dantus[b]

Department of Chemistry and Center for Fundamental Materials Research, Michigan State University, East Lansing, Michigan 48824-1322

(Received 11 May 1998; accepted 23 December 1998)

Time-resolved transient grating techniques (TG) arising from four-wave mixing (FWM) processes are explored for the study of molecular dynamics in gas-phase systems ranging from single atoms to large polyatomic molecules. For atomic species such as Ar and Xe, each TG signal shows only a peak at zero time delay when all three incident pulses are overlapped temporally. For diatomic O_2 and N_2 and linear triatomic CS_2 molecules, the TG signals exhibit ground state rotational wave packet recurrences that can be analyzed to obtain accurate rotational constants for these molecules. With heavier systems such as HgI_2, ground state vibrational and rotational wave packet dynamics are observed. Resonant excitation allows us to select between measurements that monitor wave packet dynamics, i.e., populations in the ground or excited states or coherences between the two electronic states. To illustrate these two cases we chose the $X \rightarrow B$ transition in I_2. TG measurements yield dynamic information characteristic of vibrational and rotational wave packets from the ground and excited states. Reverse transient grating (RTG) experiments monitor the time evolution of an electronic coherence between the ground and excited states which includes vibrational and rotational information as well. Early time TG signal for the polyatomic samples CH_2Cl_2, CH_2Br_2, benzene, and toluene exhibit a coherence coupling feature at time zero followed by rotational dephasing. Differences in the amplitude of these two components are related to the contributions from the isotropic and anisotropic components of the molecular polarizability. A theoretical formalism is developed and used successfully to interpret and simulate the experimental transients. The measurements in this study provide gas-phase rotational and vibrational dephasing information

Experiment

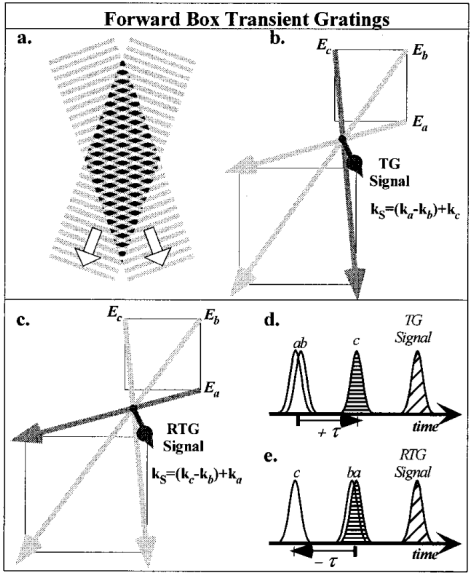

FIG. 1. Gratings formed in the forward box configuration. (a) Formation of a transient grating by two electric fields. Note that the direction of the grating bisects the angle between the fields. Areas of higher absolute electric field are darker. (b) Grating formed between E_a and E_b. Note that E_c Bragg scatters into the upper right corner resulting in the signal-beam. This occurs for $\tau \geq 0$. (c) Grating formed between E_b and E_c. Note that E_a Bragg scatters into the upper right corner resulting in the signal-beam. This occurs for $\tau \leq 0$. (d) Schematic of the pulse sequence in TG measurements. For this case, positive τ, the grating is formed by fields E_a and E_b. This signal arises from the scattering of field E_c. (e) Schematic of the pulse sequence in RTG measurements. For this case, negative τ, the grating is formed by fields E_c and E_b. This signal arises from the scattering of field E_a.

Experiment

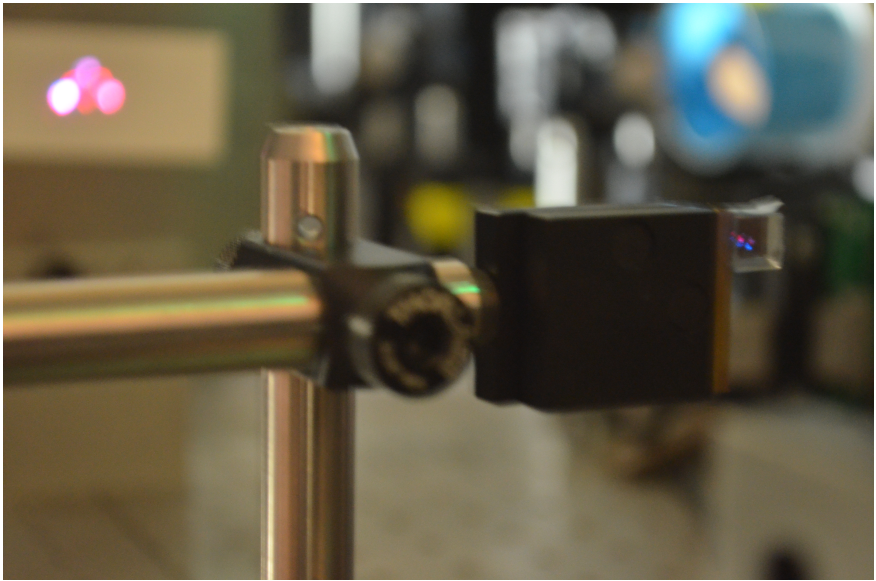

Experiment

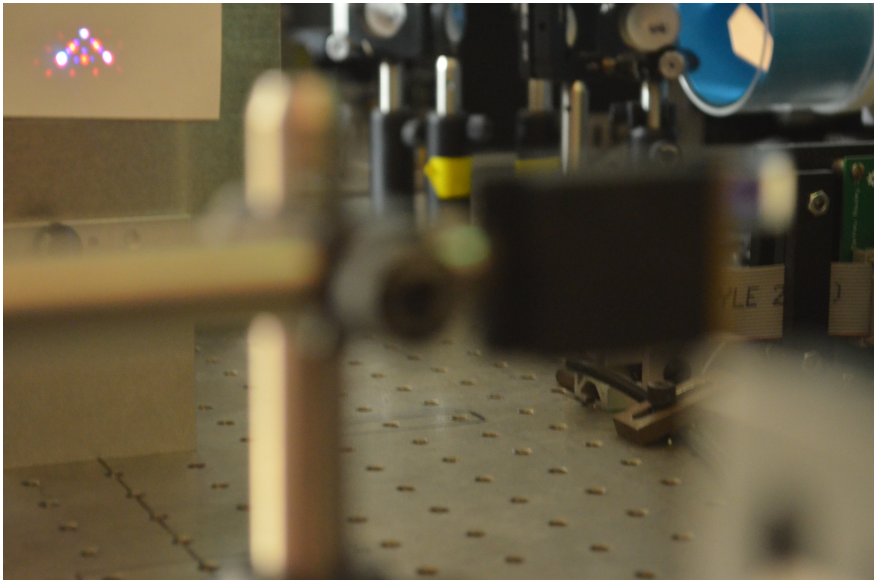

Experiment

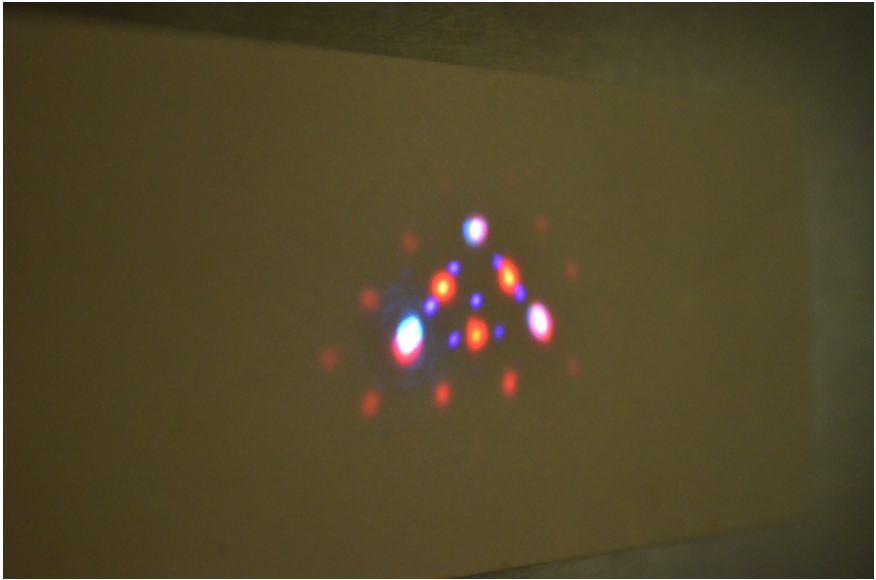

Experiment

experiment consists of measuring intensity of new beam output as function of input parameters

can control many properties of input pulses:

- color (ω)
- relative arrival time (τ)
- polarization
- intensity
- and more!

ultimately, experiments include scanning several of these parameters

challenge and opportunity in dimensionality of experiment

Gasses

gaseous reactions are particularly difficult systems

rotational-vibrational spectra of gas mixtures typically contain thousands of peaks from transitions between the many levels of the molecules

Anal. Chem. **2005,** *77,* 5467−5473

Peak Separation and Sorting by Coherent 2D Resonance Raman Spectroscopy

Peter C. Chen* and Candace C. Joyner

Chemistry Department, Spelman College, 350 Spelman Lane, Atlanta, Georgia 30314

The ability to separate and sort peaks is explored using a new coherent two-dimensional form of resonance Raman spectroscopy. This experimental technique distributes normally congested rotational−vibrational peaks along a series of curved lines according to vibrational sequence, rotational quantum number, and selection rule. Each line consists of rotational−vibrational peaks that have the same vibrational sequence and the same value for ΔJ, distributed in order by rotational quantum number. For diatomic molecules, these lines originate from points where they initially travel in opposite or orthogonal directions in two-dimensional space, which helps facilitate the separation between lines. Simulations and experimental results on C_2 in a flame confirm the ability to separate and sort these normally congested rotational−vibrational peaks. This method appears to provide a

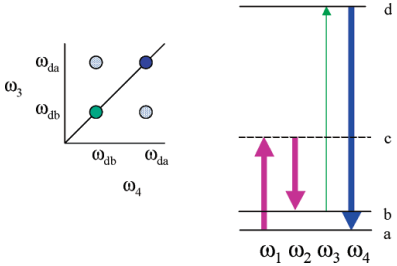

Figure 1. Simple simulated 2D plot (left) and energy level diagram (right) for C2DRR spectroscopy. The simple simulated plot shows

Gasses

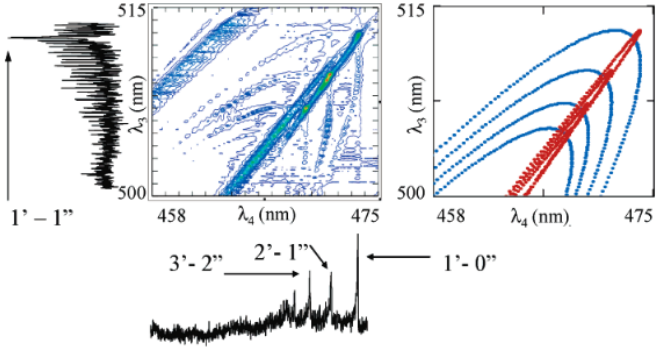

Figure 5. Experimental (left box) and simulated (right box, with $J_{max} = 75$) 2D spectra of C_2 in the Swan region shown as contour plots. The 1D spectra shown to the left and the bottom are the emission spectra from a sooty flame detected over the same λ_3 and λ_4 wavelength ranges. The spectrometer used to obtain the emission spectra had a pixel-to-pixel resolution of 0.009 nm. By comparison, the step size for the 2D experiment was 0.1 nm and the monochromator-ICCD system had a pixel-to-pixel resolution of 0.09 nm. Despite this relatively large step size and poorer resolution, the spectral resolution achieved by the 2D technique is superior to that of the 1D technique.

Drug complexing

most drugs work by physically binding to a specific site (protein, DNA, lipid)

often, drugs work simply by physically inhibiting the activity of the target

finding out what drugs bind which targets is a key part of pharmacutical development

Drug complexing

current strategies for investigating drug binding typically involve separating the bound complex(es) and testing each piece for evidence of drug binding

this is slow and disruptive—the binding properties may change as the mixture is purified

an all optical method that can identify drug binding in complex mixtures without separation would be ideal

multidimensional vibrational spectroscopy can meet this demand

Drug complexing (David Klug group)

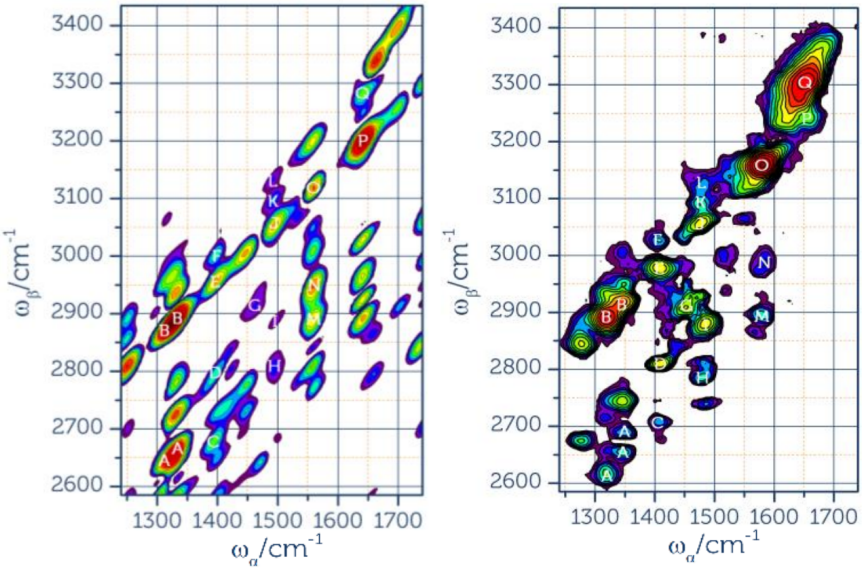

Drug complexing

100 peaks 3σ above noise floor

7 only present when drug is specifically bound

peak intensity follows expected dosing behavior

energy and anisotropy of peaks gives clues about the exact nature of the binding

measurement can be done in complex mixture including other potential targets—potentially even *in vivo*

Quantum dots

quantum dots are very small chunks of semiconductor

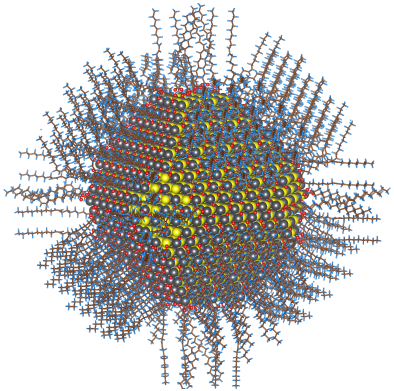

Quantum dots

quantum dots have strong electronic transitions

the energy of these transitions can be tuned by changing the size of the dot

this property makes quantum dots useful

- displays
- solar cells
- medicine

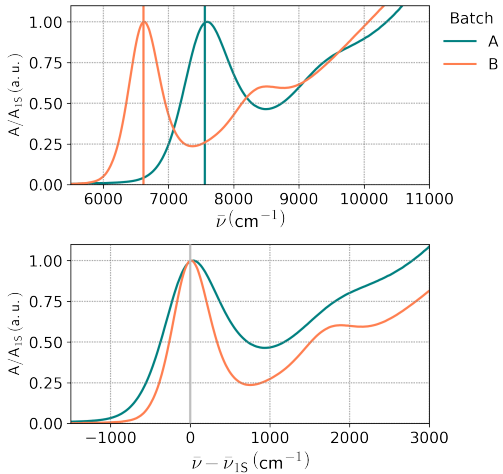

PbSe dynamics

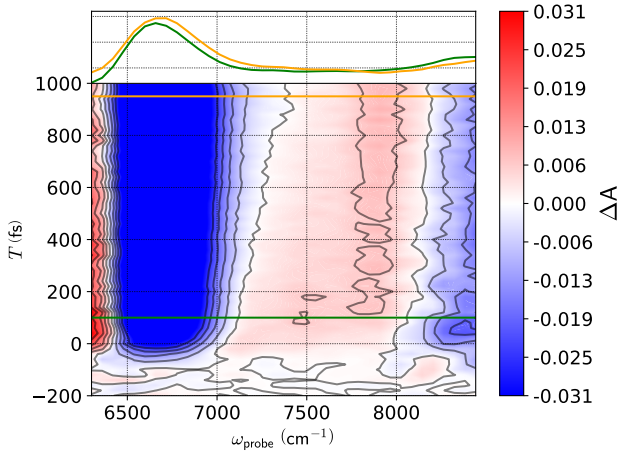

PEDOT:PSS

PEDOT:PSS is a transparent, conductive polymer

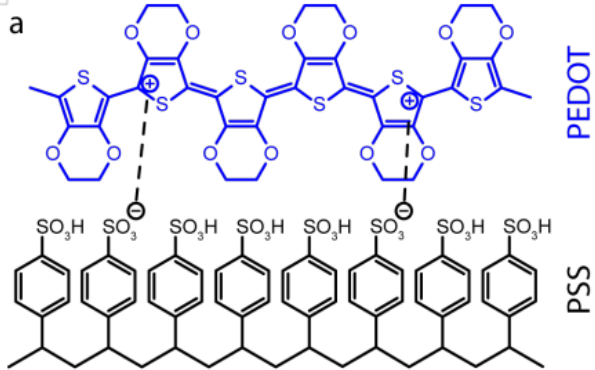

it's conductivity comes from the mobile bipolarons that it contains

PEDOT:PSS

as a polymer, PEDOT:PSS has a large amount of structural inhomogeneity

from linear spectroscopy, we know that the bipolaron transitions are broad

question: how inhomogeniously broadened are the bipolaron transitions in PEDOT:PSS?

- the answer will provide clues about the mechanism of conductivity within the polymer

Rephasing

earlier, we saw that inhomogeneity can be resolved in 2D frequency scans

it's also possible to separate inhomgeous and homogenious broadening with 2D delay scans, through a process called **repahsing** (or **echo**)

with certain pulse orderings, signal loss due to dephasing can be counteracted through echo process

PEDOT:PSS

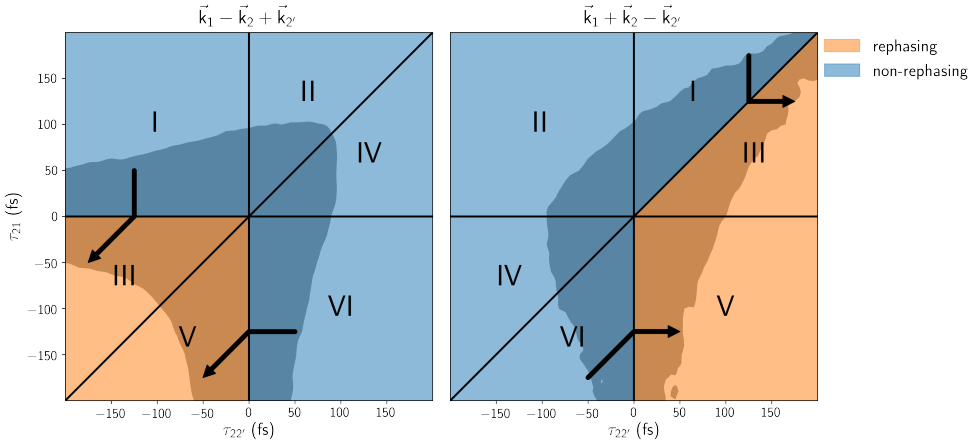
$\vec{k}_1 - \vec{k}_2 + \vec{k}_{2'}$
$\vec{k}_1 + \vec{k}_2 - \vec{k}_{2'}$
I
II
III
IV
V
VI
τ_{21} (fs)
$\tau_{22'}$ (fs)
150
100
50
0
−50
−100
−150
rephasing
non-rephasing

PEDOT:PSS

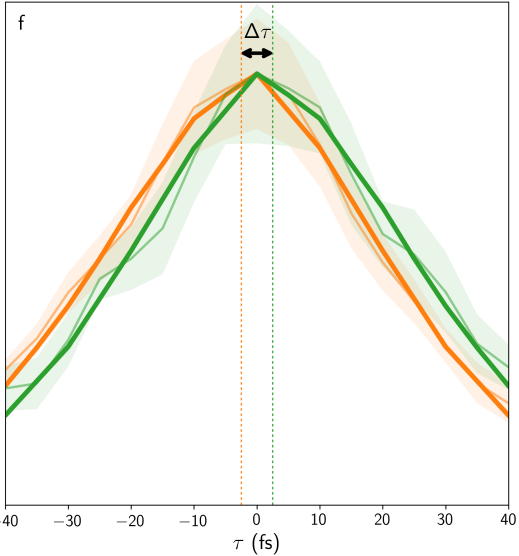

PEDOT:PSS

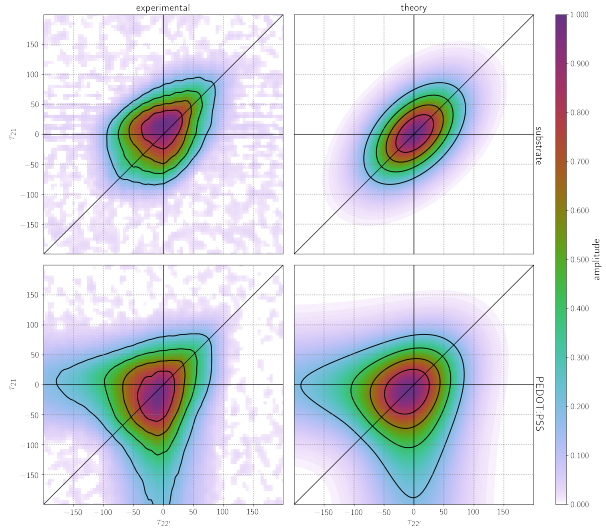

- homogeneous linewidth > 73 meV
- heterogeneous linewidth > 43 meV
- very large broadening of both kinds
- tells a story of rapidly fluctuating discrete states within PEDOT:PSS